Load Distribution in Light-Frame Wood Buildings under Experimentally Simulated Tsunami Loads

Citation	Linton, D., Gupta, R., Cox, D., & van de Lindt, J. (2015). Load Distribution in Light-Frame Wood Buildings under Experimentally Simulated Tsunami Loads. Journal of Performance of Constructed Facilities, 29(1), 04014030. doi:10.1061/(ASCE)CF.1943-5509.0000487
DOI	10.1061/(ASCE)CF.1943-5509.0000487
Publisher	American Society of Civil Engineers
Version	Accepted Manuscript
Terms of Use	http://cdss.library.oregonstate.edu/sa-termsofuse

Load Distribution in Light-Frame Wood Buildings under Experimentally Simulated Tsunami Loads

David Linton[1]; Rakesh Gupta[2], M. ASCE; Dan Cox[3], M. ASCE; John van de Lindt[4], M. ASCE

Abstract

This paper presents the results of a test program whose goal was to better understand the contribution of individual elements to the performance of typical light-frame wood structures during tsunami loading. The intent was to be able to replicate failures in a structural engineering laboratory that were observed during laboratory experiments of hydraulic loading on wood walls at the NEES Tsunami Facility at Oregon State University. The elastic and inelastic response of shear walls, out-of-plane walls, and a full light-frame wood structural system subjected to varying lateral loads were observed using Digital Image Correlation (DIC). DIC provided a non-contact, three-dimensional measurement system that returned displacement results measured at multiple areas of interest on the wall surface. Overall, these experiments show that the elastic stiffness and ultimate capacity of the shear wall is significantly higher at full height compared to intermediate heights on the wall, and the ultimate lateral capacity was higher in comparison to the a full structural system. The results indicate that the out-of-plane wall behaves like a one way slab with limited contribution from adjacent studs in carrying load. The stud to bottom plate connection failures observed during the wave tank tests were successfully reproduced, and indicate that the nailed connection needs to be reinforced to utilize the available capacity of the individual framing members.

[1]Structural Design EIT, Group Mackenzie, Portland, Oregon, 97214, USA

[2]Professor, Department of Wood Science and Engineering, Oregon State University, Corvallis, Oregon, 97331, USA; Corresponding author: rakesh.gupta@oregonstate.edu

[3]Professor, School of Civil and Construction Engineering, Oregon State University, Corvallis, Oregon, 97331, USA

[4]George T. Abell Professor in Infrastructure, Department of Civil and Environmental Engineering, Colorado State University, Fort Collins, CO 80523-1372, USA

Keywords: shear walls, light-frame, wood, walls, tsunami forces, transverse, OSB, out-of-plane

Introduction

A series of several devastating tsunamis over the past decade has highlighted the need for a better understanding of these natural disasters, and how communities can better prepare for the next tsunami. With most tsunamis originating from a subduction zone earthquake, the coastal communities of the Pacific Northwest are located in a tsunami hazard zone. The Cascadia Subduction Zone (CSZ) runs along the Pacific coast from Northern California to Vancouver Island, and there is a 14% probability that a near field tsunami will occur along the CSZ in the next 50 years (Groat, 2005). A near field tsunami along the CSZ would come from a similar fault process as the recent Japan and Chile tsunamis of 2011 and 2010 respectively, and although the size of the tsunami is uncertain, nevertheless this highlights the need for proper preparedness for these high risk communities. With a majority of buildings in the United States being wood structures, and particularly many of the coastal communities where inland tsunami inundation would occur, there is a need to better understand the performance of these structures during a tsunami event.

With the inherent limitations of testing full scale structures the majority of previous knowledge has come from field reconnaissance (Lukkunaprasit and Ruangrassamee, 2008) or small scale laboratory experiments (van

de Lindt et al., 2009). Testing full scale structures is generally limited to transverse walls in wave flumes (Linton et al., 2011, Arikawa, 2009). Due to the difficulty in testing full scale structures under tsunami loading this study focuses on simulating tsunami loading in a typical structures laboratory on a full scale wood structure. This paper presents the methods and results of full scale testing of individual light frame wood walls and a typical wood structural system in the Gene D. Knudson Wood Engineering Laboratory at Oregon State University. The purpose of this research was to further investigate how a typical light frame wood structure performs. Specific objectives for this study were:

- Evaluate the elastic stiffness of individual structural components of a light frame wood structure.
- Investigate the contribution of each component to the performance of a full structural system.
- Simulate tsunami loading in a structural laboratory and reproduce failure modes observed during hydrodynamic laboratory testing (Linton, 2012) in the tsunami testing facility at Oregon State University.

With wood shear walls being the primary lateral force resisting system in most wood structures, they have been the most heavily researched light frame wood structural component. The majority of shear wall tests have been conducted under the ASTM E564 standard (ASTM, 2000), where an individual shear wall is loaded through the top plate of the wall. This testing procedure is used to evaluate the static load capacity and deflection of wood frame walls to be used in a lateral force resisting system. Additionally wood shear walls are often tested using cyclic loading protocols to further capture the response observed during seismic events, i.e. the 1994 Northridge Earthquake. There have been numerous investigations into the contribution of fasteners, wall sheathing, hold downs, and various aspect ratios on wall capacity and stiffness. Sinha and Gupta (2009) evaluated the load and strain distributions in shear walls sheathed with both oriented strand board (OSB) and gypsum wall board (GWB) and only OSB on one side. The observed strains show load is concentrated around the fasteners on the panel edges and the strains in the field of the panel were below the detectable limit. The behavior of the load distribution in the fasteners is important for better understanding the load path of lateral

loads through the shear wall. Due to the load path observed during both wind and seismic loading the effect of lateral loads applied at intermediate heights on a shear wall has been of little importance. This capacity at intermediate heights is of much greater importance during a tsunami event because of potentially large lateral loads from debris impact.

The out-of-plane performance of wood structures is also important to resist tsunami loading, and is therefore a significant portion of this project. The majority of previous work related to out-of-plane loading on wood walls is focused on wind design. Polensek and Gromala (1984) used computer software to simulate strength and stiffness distributions of a typical wood frame wall, and concluded that they could sustain wind loads in excess of a 100 year event. Rosowsky et al. (2005) investigated the strength and reliability of wood walls subject to combined axial and transverse loads. The effect of combined loads is often over looked when determining capacities for individual wall elements. The work of Rosowsky et al. further addressed this by correlating test results with a beam-spring model typically used for modeling floor systems. Winkel and Smith (2010) also researched the effect of combined in-plane and out-of-plane loading on wood walls and observed a capacity decrease of 25 to 40% when compared to only in-plane loading. The connections of the studs to the base plate strongly influenced the overall capacity of the wall when subjected to combined loading.

The testing of full structural systems is limited due to the difficulty of testing at full scale, and is often limited to the use of finite element modeling. Martin (2010) used SAP2000 to model the load path of hurricane loads on a wood structure. Van de Lindt et al. (2010) tested a full scale six story wood frame apartment building on the world's largest shake table in Miki, Japan. The results were used to help validate the performance-based seismic design philosophy developed in the NEESWood project.

With tsunami research being primarily limited to small scale experiments, the investigation into detailed structural response has been limited and tsunami research has instead focused on quantifying tsunami forces

(Ramsden, 1996). The main source for structural performance knowledge has come from field reconnaissance (Lukkunaprasit and Ruangrassamee, 2008). Wilson et al. (2009) investigated wave loading on a 1/6th scale two-story wood-framed residential building utilizing several building configurations and test conditions. Uplift forces were measured from wave impact in both flooded and non-flooded conditions. From this a qualitative analysis showed that differences in structural stiffness of components can cause different load distributions in the structure. Garcia (2008) used an identical $1/6^{th}$ scale model as Wilson et al. to calibrate a SAPWood computer model, which was then used to calculate the internal building forces based on the measured displacements from the wave tank tests. Garcia concluded that the force coefficient of 4.5 used in the Honolulu Building Code was an order of magnitude higher then those observed during the tests, and the flexibility of the compliant structure contributed to lower impact forces. Arikawa (2009) tested both concrete and wood walls in a wave flume, and concluded that a 2.5 m off shore tsunami would cause the wood walls to fail. Linton et al. (2011) also tested full scale wood walls in a large wave flume, and observed both wall performance and measured wave impact forces. The results showed that the linear momentum equation for steady flow assumptions did a good job of predicting the tsunami wave forces. Linton et al. also observed increased wall flexibility resulted in lower transient forces, but didn't affect the quasi-static forces measured on the wall.

Materials and Methods

Specimens

All test specimens were designed in accordance with the prescribed sections of the 2008 Oregon Residential Specialty Code (ICC, 2008), and were constructed using No. 2 and better grade 38 x 140 mm (2 x 6 nominal size) kiln dried Douglas-fir dimension lumber. Specimen 1 was a 2.44 x 2.44 m shear wall with double top plates and double end studs at one end as shown in Fig. 1. Specimen 2, out-of-plane (OOP) wall, was the same size as specimen 1, but had two end studs (one flat) as shown in Fig. 2. Specimen 1 had a single stud at one end of the wall, that when combined with the two stud corner of specimen 2 is a typical three stud corner used in residential construction (ICC, 2008). This was used to more accurately represent current building practices.

For both wall specimens 1 and 2 the vertical studs were spaced at 0.40 m on center (o.c.), and were vertically sheathed with two 1.22 x 2.44 m x 11.1 mm 24/16 APA rated OSB panels. The double end studs and double top plates were face nailed at 610 mm o.c. with two 10d (3.3 x 75 mm) framing nails. Specimen 3 is a 2.44 x 2.44 m diaphragm with joists spaced at 0.61 m and sheathed with two 1.22 x 2.44 m x 18.3 mm sized for spacing struct-I-floor APA rated tongue and groove plywood. All stud and joists were end nailed with three 16d (3.3 x 82.6 mm) nails per connection. Sheathing panels were connected to the framing using 8d (2.9 x 60 mm) nails spaced 0.15 m o.c. along the panel edges and 0.31 m o.c. in the field. All framing nails were full round head, strip cartridge, and smooth shank nails that were driven using a pneumatic nail gun. Table 1 outlines the details for each specimen, a total of seven shear walls, three OOP walls, and one diaphragm were used.

Test Setup

There were two different primary test setups used during these experiments. Setup 1 consisted of a single shear wall (Specimen 1, Table 1) bolted to a steel floor beam (foundation) as shown in Fig. 3. An additional steel beam (lateral restraint) was connected to the top plates with two 12.7 mm A307 bolts and was laterally braced to the strong wall. Setup 1 was used for the "Shear Wall" tests (SW1-5, Table 2). Setup 2A-C (Table 2) used two shear walls, an OOP wall (Specimen 2, Table 1), and a diaphragm (Specimen 3, Table 1) configured in a full structural system shown in Fig. 4 and Fig. 5. For setup 2 the diaphragm was connected to the top plates of the shear walls using Simpson H1 brackets at each joist, and Simpson HGA10KT brackets in-between each joist connected to the rim board. The HGA10KT brackets were used instead of toe nails to make it easy to change out specimens. Three different variations of setup 2 were used during testing. In all three variations the shear wall and diaphragm were connected together as discussed above. In the first variation, setup 2A, the OOP wall was isolated from the system by two load cells as shown in Fig. 4. The top corners of the OOP wall were attached to an 8.9 kN (2 kip) load cell at the top corner of each shear wall. Setup 2A was laterally restrained to the strong wall because the OOP wall didn't provide lateral support. For the second variation, setup 2B, the OOP wall was connected to the SW, but the diaphragm was not connected to the top plate of the OOP wall. Setup 2C was the same as setup 2B; however, the diaphragm was connected to the top plate of the OOP wall using three evenly

spaced HGA10KT brackets. Fig. 4 shows setup 2C with the SW, OOP wall, and diaphragm all connected into a full system. The OOP wall was connected to a steel floor beam (foundation) using two 12.7 mm A307 bolts spaced at 1.83 m. Neither setup 2B nor 2C were laterally restrained.

These setups were used to show the individual influence of each component in a full structural system as each subsequent setup has more complicated boundary conditions. Setup 1 allowed for analysis of the individual shear wall, setup 2A isolated the OOP wall, setup 2B added in the SW and OOP wall corner boundary condition, and finally setup 2C included all three components working in a system.

Experimental Process

Individual shear walls (setup 1) were loaded in-plane at eight locations that correspond to increments of 0.31 m (1 ft) along the height of the wall, see Fig. 3. Elastic stiffness tests were performed where a single point load was applied at a rate of 2.54 mm/min (0.1 in/min) until a force of approximately 1.78 kN (400 lbf) was reached. Following the elastic tests a series of monotonic failure tests were performed on the shear walls at 0.61 m (2 ft) height increments. The failure tests were performed at a rate of 7.62 mm/min (0.3 in/min) to help maintain acceptable data acquisition and analysis. SW1 and SW5 are identical experiments, it was necessary to repeat the failure test due to improper setup of the load cell during SW1.

Following the SW tests a series of elastic stiffness experiments, “OOP1” (setup 2A), “OOP2” (setup 2B), and “OOP3” (setup 2C), using the same loading protocol were performed on the structural system of setup 2. For each of the OOP experiments the OOP wall was loaded with a point load normal to the surface, and was repeated at twenty different locations shown in Fig. 5. The twenty load locations were as follows: the edge of the wall (grid A) at the same eight heights from the SW experiments; and three interior studs (grids B-D) at height increments of 0.61 m (2 ft) on each stud. All heights are measured from the bottom of the wall. Note that

the load location for each trial is labeled with the alphabetical grid and height, i.e. B4 or A7. The targets are labeled in Fig. 5. Table 2 outlines the setup, specimens used, number of trials, and load locations for experiment.

After the OOP tests two different failure tests, “FAIL1” and “FAIL2”, were performed on the complete structural system (setup 2C). FAIL1 consisted of a horizontal distributed load applied across the middle three studs (grids C, D, E), normal to the OOP wall at 0.61 m (2 ft) above the base of the wall. A steel HSS section, shown in Fig. 6, was attached to the hydraulic actuator to simulate a distributed load. FAIL2 was a point load applied at the corner of the diaphragm (A8), shown in Fig. 7, is similar to the monotonic shear wall tests discussed above. Both tests were performed at a rate of 7.62 mm/min (0.3 in/min).

Data Acquisition

Recall that a major objective of this test program was to load the specimens such that failure mechanisms observed during hydrodynamic testing were replicated in the structural laboratory. To quantitatively determine this, stress and strain measurements were measured using an optical measurement system, VicSnap, which used two cameras setup on a tripod to capture a time series of photos. The cameras were externally triggered and connected to a computer where images were saved and external data from the load cells and hydraulic actuator displacement were recorded. The images were then analyzed using digital image correlation (DIC) proprietary software, Vic 3D (Correlated Solutions Inc., 2010), where a small subset of pixels were mathematically correlated with the base image (zero load) to get the 3D deflection data for each target. The data was then exported and processed in Excel and Matlab. Targets were used to provide an easily identifiable high contrast pixel area within the desired image area to measure the deflection of specific locations on the wall as shown in Fig. 5.

Digital image correlation has been used primarily for small scale stress and strain measurements (Choi et al., 1991), but have more recently been used for large scale experiments (Sinha and Gupta, 2009). Sinha and Gupta (2009) used a similar DIC setup to measure strain distribution in full scale wood walls, and successfully

showed that the use of DIC on large scale specimens can provide accurate measurements. The use of DIC was advantageous for the scope of this project because it allows for accurate tracking of multiple areas of interest on the walls that would otherwise need to be individually instrumented.

In addition to the stress/strain measurements, the specimens were loaded using a 44.5 kN (10 kip) hydraulic actuator attached to a strong wall and supported by a ratchet strap. The hydraulic actuator had a 0.15 m total stroke, and was controlled by an MTS 406 servo controller. Attached to the hydraulic actuator was a 111.2 kN (25 kip) load cell with a sampling rate of 1 Hz.

Results and Discussions

Shear Wall Performance

The individual shear walls tested in setup 1 were loaded with low level forces to remain elastic, as well as to failure. Setup 1 was used to allow comparison to typical monotonic shear wall tests. Fig. 8 shows an example load vs. deflection plot from the elastic load test, SW5 Trial05, where the load was applied at grid H5. The results from the elastic tests are shown in Fig. 9, which shows the average stiffness along the height of the shear wall. The average stiffness was calculated from the load vs. local deflection plots when the load was applied at the specific height. From Fig. 9 we can see that the shear wall has significantly more stiffness when load is applied to the top plate than anywhere else along the height of the wall. This result would be expected because the load path for load at grid 8 vs. grids 1-7 is different. The load at grid 8 is transferred through the top plates into the nails (approximately 30) around the top edges of both OSB panels, before being transferred through shear in the panel to the perimeter studs and bottom plate. In the case of loads at grids 1-7 the stud is loaded in bending with the sheathing nails acting as spring elements. In this case the majority of force is concentrated into only a few nails nearest the load. Also contributing to the total deflection is the rotation of the stud. With OSB sheathing only on one side an unbalanced loading condition exists where there are only nails resisting the applied load on one side of the studs, causing torsion in the stud. The combination of stud rotation and fewer nails sharing load results in lower stiffness values along the height of the wall.

A similar trend discussed above from the elastic tests is continued with the failure tests at grids 2, 4, 6, and 8. Fig. 10 shows the load vs. deflection curves for the failure tests from SW2 (grid 2), SW3 (grid 6), SW4 (grid 4), and SW5 (grid 8). The data from SW1 was not plotted because the load cell was improperly setup and maxed out before the wall failed. Similar to the elastic stiffness results from Fig. 9 the intermediate grids (2-6) show significantly lower capacities compared to grid 8. The sudden drop in load for SW3 was a result of the top plate splitting at the stud end nail farthest from the OSB sheathing. Due to the stud rotating this particular nail was highly stressed and caused the top plate to split, shown in Fig. 11.

The results from Fig. 9 and Fig. 10 are important when engineers start to consider debris impact loads during a tsunami event. Unlike a typical concrete or masonry shear wall, the wall has different load path characteristics and performs much different at intermediate wall heights compared to the full height considered for typical lateral load design. The overall structural system could be sufficient to withstand the wave impact, but insufficient for local concentrated loads from debris. The addition of blocking between studs at these locations could help transfer the load into the sheathing and subsequently increase the available capacity.

The inclusion of setup 2C in this testing provided a unique opportunity to compare the performance of an individual shear wall with a full structural system when loaded with a point load at the diaphragm level. Fig. 12 shows the load vs. deflection curves from failure experiments SW5 (setup 1) and FAIL2 (setup 2C). Due to different DIC camera positions for these two setups the displacements *u*, *v*, and *w* from the global directions *x*, *y*, and *z* don't correspond, so the results were transferred to a similar set of displacement coordinates $\delta 1$, $\delta 2$ and $\delta 3$. These coordinates are shown in Fig. 3 for SW5 and Fig. 5 for FAIL2. The three load vs. deflection curves in Fig. 12A correspond to the horizontal ($\delta 1$) and vertical ($\delta 2$) in-plane displacement and out-of-plane ($\delta 3$) displacement for an individual shear wall (setup 1) loaded at grid 8 (SW5 Trial 09). Fig. 12B shows the same load vs. deflection curves for a full structural system (setup 2) loaded at grid A8 (FAIL2). The full structural

system performed quite a bit differently than the individual shear wall, because it was not laterally braced. The horizontal in-plane deflection ($\delta 1$) in Fig. 12B is similar, but the full system only carried about 90% of the ultimate load compared to the individual shear wall. The full system had about three times the amount of out-of-plane deflection; whereas the individual shear wall was laterally restrained and had very little out-of-plane deflection. With the full system only being laterally restrained by the out-of-plane wall, with the increased out-of-plane deflection there was significantly less vertical deflection (Fig. 12, $\delta 2$) compared to the laterally restrained shear wall. Fig. 7 shows the deflected shape of the full structural system at maximum extension of the hydraulic actuator.

Out-of-Plane Wall

The contribution of individual structural elements (shear wall, OOP wall, and diaphragm) were investigated using OOP1 (setup 2A), OOP2 (setup 2B), and OOP3 (setup 2C) experiments. Similar to the shear wall experiments the elastic stiffness was measured at twenty locations on the OOP wall. Fig. 13 shows the stiffness for vertical grids B-D, which correspond to the wall studs shown in Fig. 5, and also includes the calculated stiffness for each location using an idealized simply supported beam model. The vertical axis corresponds to the horizontal grids 2-8. Fig. 14 shows the local out-of-plane deflections from OOP3 Trial09, where the wall was loaded at D2 with 1.71 kN.

The results from Fig. 13 indicate that there doesn't appear to be any significant interaction between adjacent studs or at the wall corner. The measured stiffnesses in Fig. 13 compare well to a simplified beam deflection model leading to the conclusion that the OOP wall stiffness is directly related to the stiffness of each individual stud and therefore the wall can be idealized like a one way slab with the load going through each individual stud into the top or bottom plate like a simply supported beam and then into the shear wall. This is also shown with all three grids having similar stiffness profiles, further lending to the observation that there isn't any additional stiffness gained from the OSB sheathing and adjacent studs. The stiffness values for OOP3 are very similar to the values for both OOP1 and OOP2, which shows that at the low forces used during these

experiments the diaphragm has little or no contribution to the stiffness. This is most likely because the stiffness of the double top plate is much greater than the flat bending stiffness of the 2x6 rim board, resulting in the top plate carrying the entire load at the low forces used during these experiments. Another contributing factor could be the small amount of slop in the connections between the diaphragm and top plate.

The results from an individual trial, OOP3 Trial09, shown in Fig. 14 also supports the conclusion there is very limited contribution from adjacent studs when out-of-plane load is applied on the wall. When the load was applied at D2, we get the largest deflections at D2, with decreasing local deflections along the height of grid D. The other three adjacent studs have minimal deflections, which can likely be attributed to deflection of the top plate and some inherent looseness in the anchor bolt connection to the foundation.

These results are important for engineers, because it validates the common assumptions that out-of-plane walls can be treated as a simply supported beam element. This assumption makes the analysis of out-of-plane walls quick and easy. When looking at the effects of concentrated loads, it is unrealistic to distribute loads over an area larger than the contact area because there is no significant load sharing between adjacent studs.

Experimentally Simulated Failures

The failures of the out-of-plane wall stud to bottom plate connection that were observed during laboratory experiments in the Large Wave Flume at Oregon State University (Linton, 2012) were reproduced during two trials of the FAIL1 experiment. Fig. 15 shows the failures from Trial01 (Fig. 15A) and Trial02 (Fig. 15B). During each trial the same connection failure observed during the wave tank tests was successfully reproduced in the FAIL1 experiment. The loads vs. deflection results from both trials are shown in Fig. 16. The deflection is the average from grids C2, D2, and E2. The small drop in load at approximately 20 mm of deflection for Trial01 was from the stud splitting at the connection as shown in Fig. 15A. The observed failures are important because it shows that in order to improve the performance of light-frame wood structures during a tsunami event the stud to bottom plate connection needs to be strengthened. This connection could be easily improved with the addition

of a simple metal bracket, with many different options available that are common in wood construction. With this connection properly secured the load path would be complete between the studs and bottom plate, thus allowing for more efficient use of the available capacity of the full structural system.

Summary and Conclusions

This study focused on the performance of full scale individual elements of light-frame wood construction, as well as a full structural system. Under a series of both elastic and inelastic load cases the elastic stiffness and ultimate load capacities were observed, with the following conclusions drawn from this study:

1. Both the elastic stiffness and ultimate load capacity were much greater at the full height of the shear wall compared to the other three intermediate heights.
2. The monotonic capacity of the shear wall when included in a full structural system was less compared to the same shear wall with the top of the wall laterally braced, because the wall was able to move both in-plane and out-of-plane as the load was applied.
3. The elastic stiffness and local deflections observed during the “OOP” experiments show that the out-of-plane wall behaves like a one way plate with very limited interaction between adjacent studs.
4. At the low force levels in these experiments it was also shown that the diaphragm provided negligible increase in the out-of-plane wall stiffness, most likely due to the irregularities in the construction of the diaphragm to wall connections.
5. The structural failures observed during the hydrodynamic laboratory experiments at the tsunami testing facility at Oregon State University were successfully reproduced. To improve the performance of light-frame wood structures during a tsunami event, it is necessary to increase the shear capacity of the nailed connection of the studs to the bottom plate along the out-of-plane wall.

The results and observations from this study provide important information towards improving the design of light-frame wood structures to better protect the lives of occupants and mitigate structural damage during a tsunami event. The successfully simulation of failures observed during hydrodynamic testing also provides an

avenue to expand tsunami simulation testing in a structural laboratory, helping to expand the available resources for researching structural performance during a tsunami.

Acknowledgements

This research was supported by the National Science Foundation under Grant No. CMMI-0830378. The opinions and statements in this paper are those of the authors and do not necessarily reflect those of the NSF. The authors thank Milo Clauson and the Gene D. Knudson Wood Engineering Laboratory staff for their assistance in this project.

References

Arikawa, T. (2009). "Structural Behavior Under Impulsive Tsunami Loading." *Journal of Disaster Research*, 4 (6), 377-381.

ASTM. (2000). "Standard method of static load test for shear resistance of framed walls for buildings." *ASTM E 564-00*, West Conshohocken, Pa.

Choi, D., Thorpe, J., Hanna, R. (1991). "Image analysis to measure strain in wood and paper." *Wood Science and Technology*, 25(4): 251-262.

Correlated Solutions Inc. (2010). *Vic 3D user's manual*, West Columbia, S.C.

Garcia, R.A. (2008). Wave and Surge Loading on Light-Frame Wood Structures." MS thesis. Colorado State University, Fort Collins, Coloarado.

Groat, C.G. (2005). Statement of C.G. Groat, Director US Geological Survey, US Department of the Interior, Before the Committee of Science, US House of Representatives, January 26.

International Code Council (ICC). (2008). *2008 Oregon Residential Specialty Code*, Country Club Hills, IL.

Linton, D. (2012). "Tsunami Loading on Light-Frame Wood Structures." MS thesis. Oregon State University, Corvallis, Oregon.

Linton, D., Gupta, R., Cox, D., van de Lindt, J., Oshnack, M.E., Clauson, M. (2011). "Evaluation of Tsunami Loads on Wood Frame Walls at Full Scale." *Journal of Structural Engineering*, (in preparation).

Lukkunaprasit, P. and Ruangrassamee, A. (2008). "Building damage in Thailand in the 2004 Indian Ocean tsunami and clues for tsunami-resistant design." *The IES Journal Part A: Civil & Structural Engineering*, 1(1): 17-30.

Martin, K. (2010). "Evaluation of System Effects and Structural Load Paths in a Wood-Framed Structure" MS thesis. Oregon State University, Corvallis, Oregon.

Polensek, A. and Gromala, D. (1984). "Probability Distributions for Wood Walls in Bending." *Journal of Structural Engineering*, 110(3): 619-636.

Ramsden, J. (1996). "Forces on a Vertical Wall Due to Long Waves, Bores, and Dry-Bed Surges." *Journal of Waterway, Port, Coastal, and Ocean Engineering*, 122 (No. 3), 134-141.

Rosowsky, D., Yu, G., Bulliet, W. (2005). "Reliability of Light-Frame Wall Systems Subject to Combined Axial and Transverse Loads." *Journal of Structural Engineering*, 131(9): 1444-1455.

Sinha, S. and Gupta, R. (2009). "Strain Distribution in OSB and GWB in Wood-Frame Shear Walls." *Journal of Structural Engineering*, 135(6): 666-675.

van de Lindt, J., Gupta, R., Cox, D. T., Wilson, J. (2009). "Wave Impact Study on a Residential Building." *Journal of Disaster Research*, 4(6):419-426.

van de Lindt, J., Pei, S., Pryor, S., Shimizu, H., Isoda, H. (2010). "Experimental Seismic Response of a Full-Scale Six-Story Light-Frame Wood Building." *Journal of Structural Engineering,* 136(10): 1262-1272.

Winkel, M. and Smith, I. (2010). "Structural Behavior of Wood Light-Frame Wall Subjected to In-Plane and Out-of-Plane Forces." *Journal of Structural Engineering,* 136(7): 826-836.

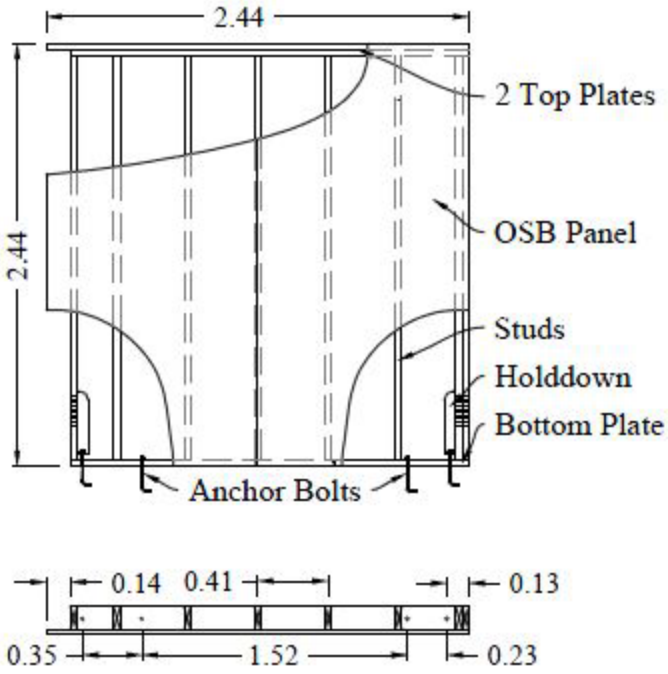

Fig. 1: Shear wall (specimen 1) schematic (dimensions in meters)

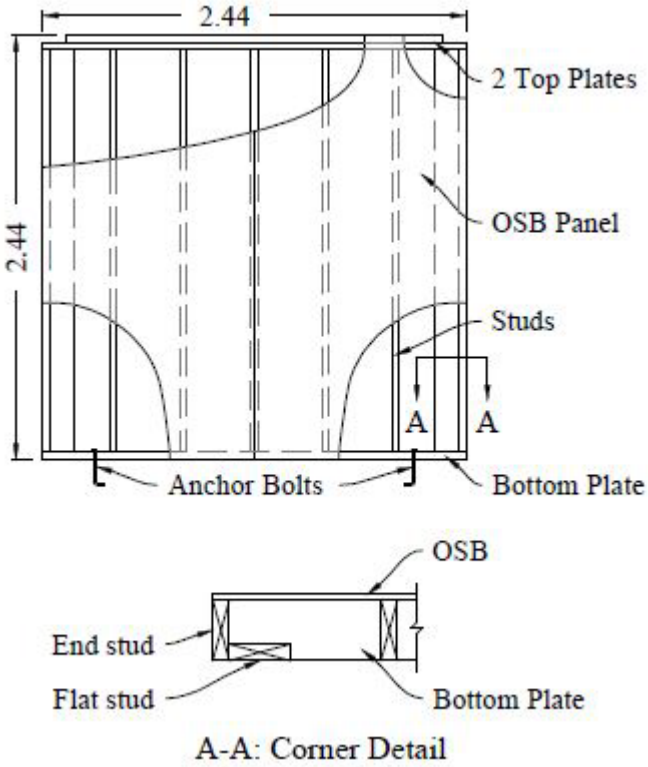

Fig. 2: Out-of-plane wall (specimen 2) schematic (dimensions in meters)

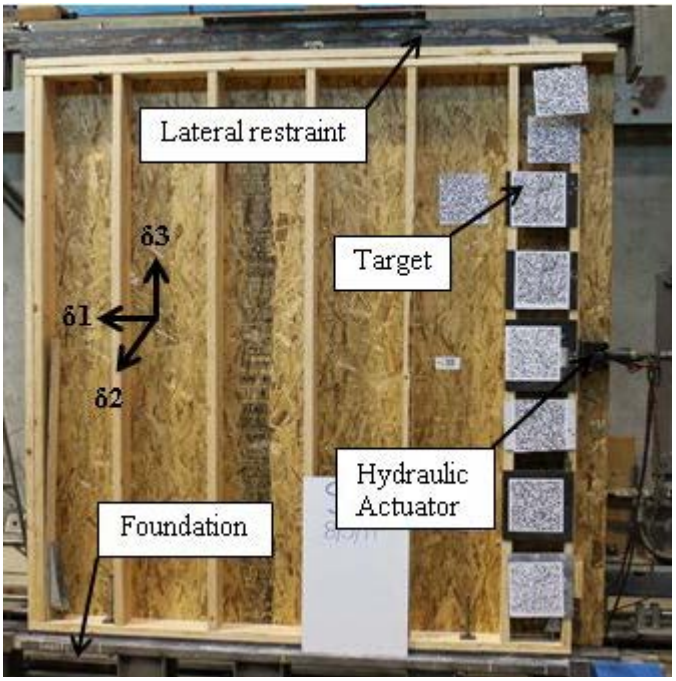

Fig. 3: Setup 1 setup (shear wall)

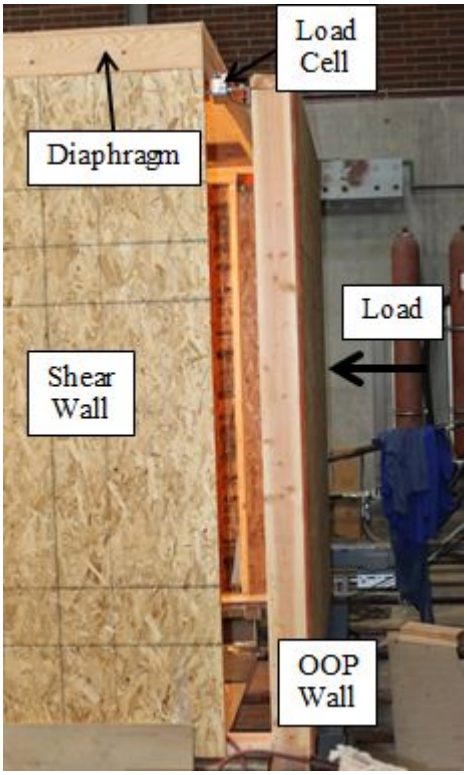

Fig. 4: Setup 2A (OOP1)

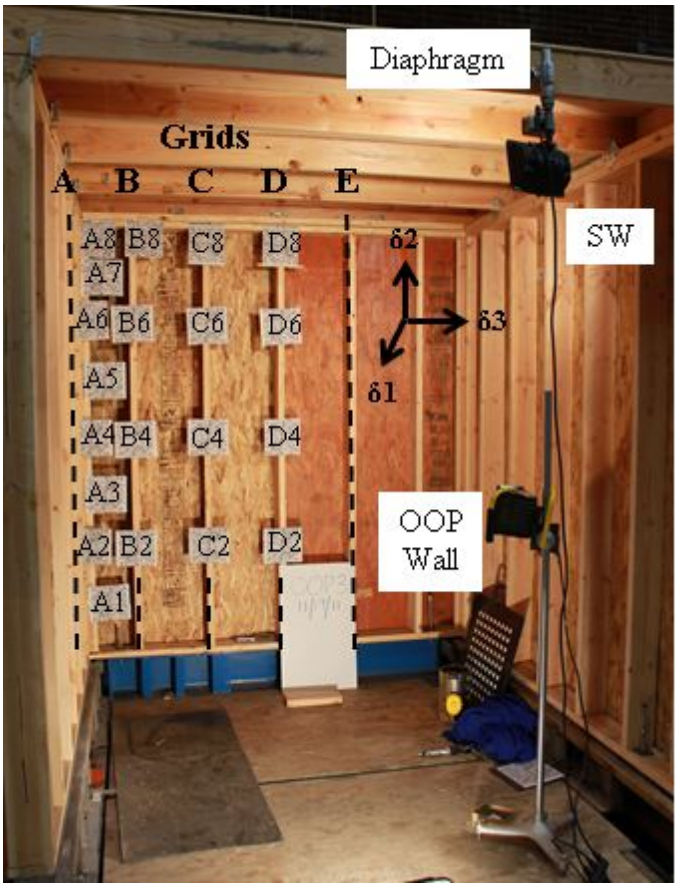

Fig. 5: Test setup 2C with grids and targets

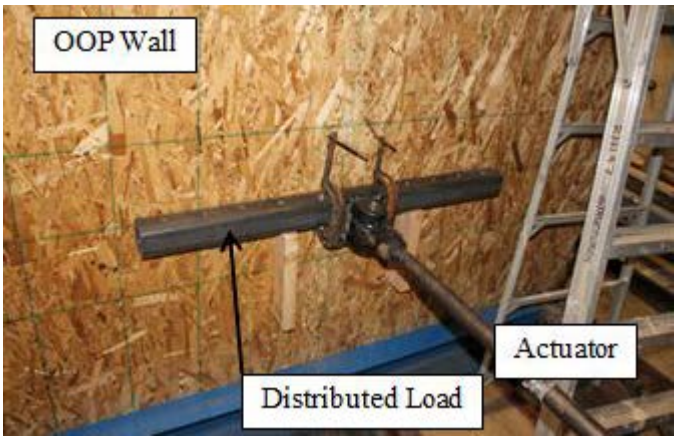

Fig. 6: FAIL1 loading setup

Fig. 7: FAIL2 loading setup

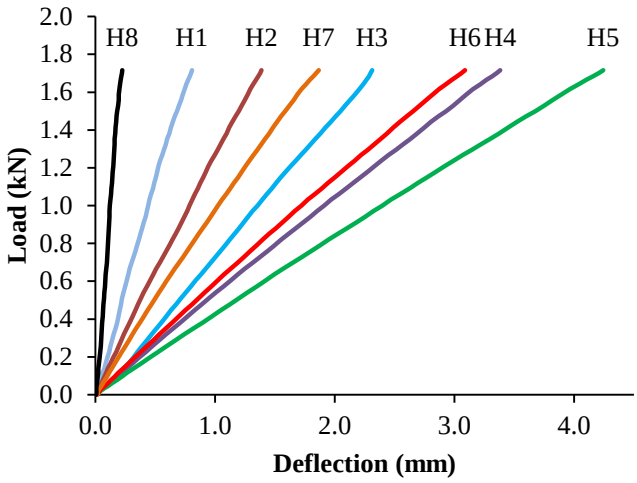

Fig. 8: Example data (SW5_Trial05)

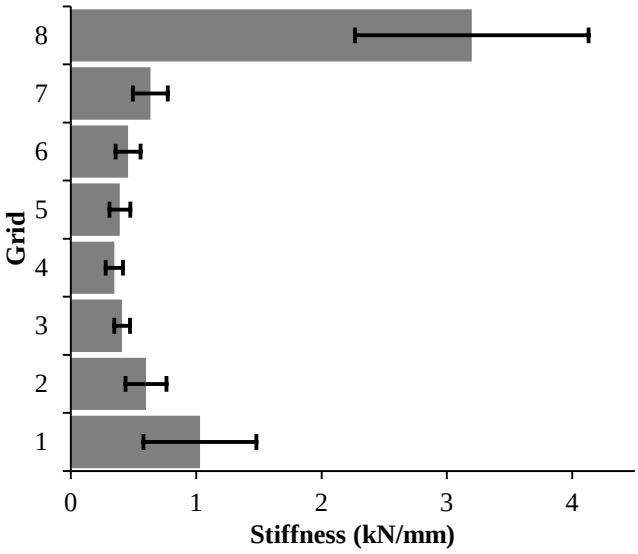

Fig. 9: Shear wall stiffness along wall height

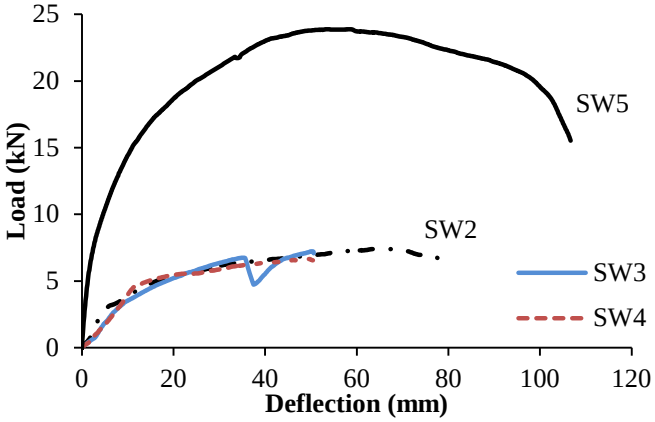

Fig. 10: Shear wall load vs. deflection curves

Fig. 11: Top plate splitting at stud connection

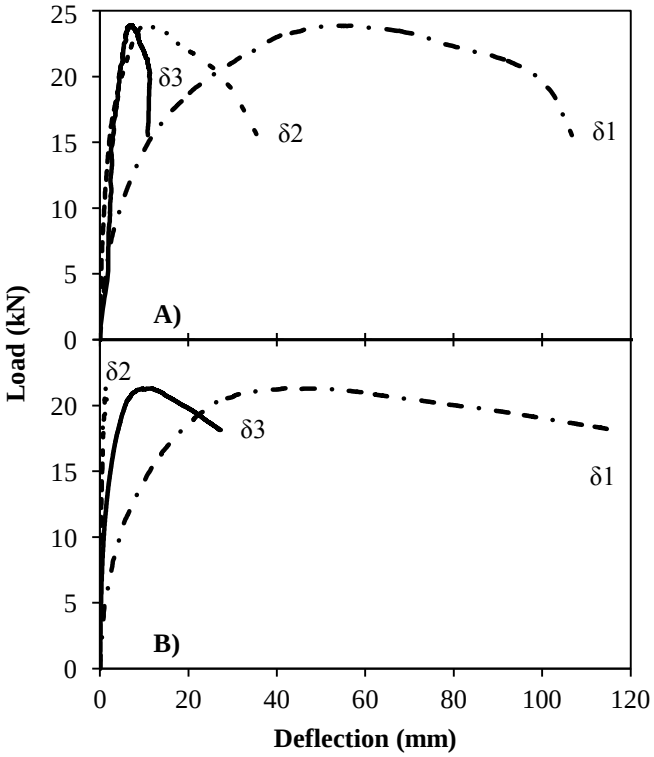

Fig. 12: Load vs. deflection curve at shear wall corner for A) setup 1 and B) setup 2C

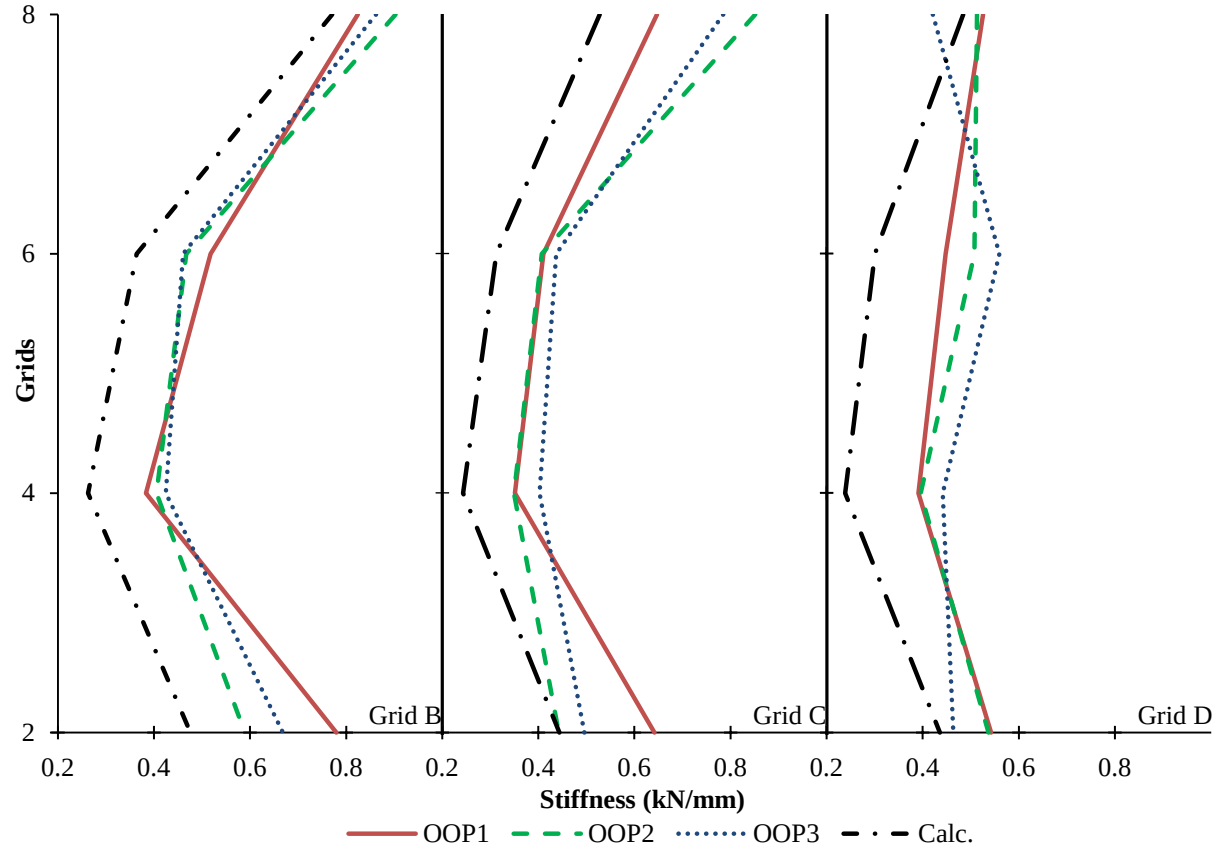

Fig. 13: Out-of-plane stiffness for experiments OOP1, OOP2, OOP3

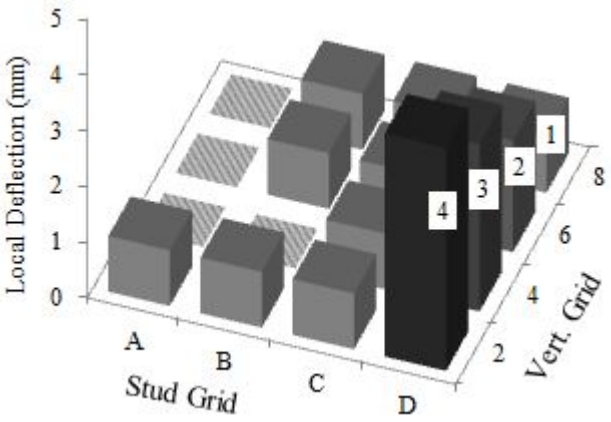

Fig. 14: Local deflections for experiment OOP3 Trial09 (setup 2C) with load applied at D2

Fig. 15: FAIL1 failures: A) Trial 01 stud splitting, B) Trial 02 stud to bottom plate connection failure

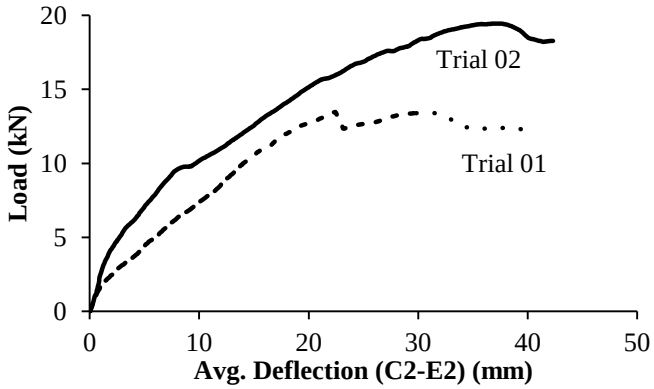

Fig. 16: Load vs. average deflection plot for FAIL1 experiment

Table 1: Specimen Information

Specimen -	I.D. -	Spacing (mm)	Sheathing -
Specimen 1A,B,C,D,E,F,G	Shear Wall	406	11.1 mm OSB
Specimen 2A,B,C	OOP Wall	406	11.1 mm OSB
Specimen 3A	Diaphragm	610	18.3 mm Plywood

Table 2: Experiment details

Test Setup	Test Name	Specimens Used	Trials	Test Description	Fail Test
1	SW1	1A	13	load at 1-8 ft and failure test @ 8'	Y
"	SW2	1B	9	load at 1-8 ft and failure test @ 2'	Y
"	SW3	1C	9	load at 1-8 ft and failure test @ 6'	Y
"	SW4	1D	9	load at 1-8 ft and failure test @ 4'	Y
"	SW5	1E	9	load at 1-8 ft and failure test @ 8'	Y
2A	OOP1	1F,1G,2A,3A	23	load at 20 grid points	N
2B	OOP2	1F,1G,2A,3A	20	load at 20 grid points	N
2C	OOP3	1F,1G,2A,3A	21	load at 20 grid points	N
2C	FAIL1	1F,1G,2A,3A and 1F,1G,2B,3A	2	load across C to D at 2ft	Y
2C	FAIL2	1F,1G,2C,3A	1	load at A8	Y